

Experimental Determination and Optimization of Hard Turned Austempered Ductile Iron (ADI) With AL-TI-N Coated Carbide Insert

Rajesh S^{*1} Veerapandian R² Madhan Kumar S³ Hari Krishnan M⁴ Vignesh T³

¹ Assistant Professor, Department of Mechanical Engineering, RMK Engineering College, Chennai.

² Assistant Professor, Department of Mechanical Engineering, SVS College of Engineering, Coimbatore.

³ Assistant Professor, Department of Mechatronics Engineering, Sri Krishna College of Engineering and Technology, Coimbatore.

⁴P. G Scholar, Government college of Technology, Coimbatore

Abstract

In this study, the effects of cutting tool insert on surface roughness, cutting force and interface temperature are investigated at varying cutting speed, depth of cut and feed rate. Hard turning process is carried out for three different cutting speeds (55,85,122 m/min), depth of cut (0.5,1,1.5 mm), and feed (0.1, 0.2 ,0.3 mm/rev). Taguchi method is used to find the optimum cutting parameters in hard turning. The orthogonal array and Signal to noise ratio are employed to study the performance characteristics in turning operation of austempered ductile iron with 32 HRC. Optimal cutting parameters for each performance measure were obtained and the experimental results are provided to illustrate the effectiveness of this approach.

Keywords: Cutting force, surface roughness, austempered ductile iron (ADI), feed rate, depth of cut

INTRODUCTION

Austempered ductile iron (ADI) was studied thoroughly in the late 1970s. ADI offers excellent characteristics of strength, ductility and toughness. It is also providing excellent fatigue strength and wear resistance [1-6]. ADI is better than forged aluminium with respect to weight to strength ratio. Higher strength and hardness of ADI have caused many researchers and engineers to doubt the machinability of this material [8]. Some issues of interest for automated tool breakage detection are: limit learning capability, exhibility problems in Computer Numerical Control (CNC) or Numerical Control (NC) controller, including relatively large dynamic errors; instability effects in the controller; the noise problem of the sensor technique; variability effects of different machining processes; and vibration effects of different environments (laboratory and factory). In spite of all these problems, the advantages of automated tool breakage detection systems still outweigh those of a manual approach. With the use of tool breakage detection in machine tools, one is able to increase machine tool life, reach a zero-defect rate, and utilize the unmanned manufacturing environment fully. Without the use of compliance in tool monitoring systems, automation of many machining processes would be simply impossible.

Hard Turning:

The turning of material with hardness greater than 35HRC, has become economically, environmental and technically viable. Hard turning is a competitive finishing process for the manufacturing precision mechanical components, the hard-turning process is similar enough to conventional turning that the introduction of this process into the normal factory environment can happen with relatively small operational changes when the proper elements are addressed. Hard turning is best accomplished with the cutting inserts made from carbide [13].

The Taguchi method has become a powerful tool in the design of experiment methods for engineering optimization of a process. The S/N ratio characteristics can be divided into two categories when the characteristic is continuous:

Smaller the better characteristics:

$$S/N = -10\log_{10} \left(\frac{1}{n} \sum y^2 \right)$$

Larger the better characteristics:

$$S/N = -10\log_{10} \left(\sum \frac{1}{y^2} \right)$$

Where y is the average of observed data, n the number of observations.

Experiment Details:

In the present investigation, the experiments were performed on MTAB SIMENS 802C CNC is shown in fig 1



Figure 1. MTAB SIMENS 802C CNC

Work Piece Material

The material employed in this study is Austempered ductile Iron (ADI). Specimens were prepared under different austenizing temperature and austempering temperatures. Specimens were prepared at austenised 920° C for 100 min and then austempered in a salt bath at 400° C for 100 min. The final dimensions of the cylindrical work piece are 150 x 50 mm. Its density is 7.22g cm³. The chemical composition of Austempered Ductile Iron is shown in the table 1.

Table 1. Chemical composition of Austempered Ductile Iron.

| Composition | C | Mn | Si | S | P | Cr | Cu | Mg |
|-------------|------|------|------|-------|-------|------|------|------|
| % | 3.66 | 0.21 | 2.76 | 0.021 | 0.011 | 0.05 | 0.28 | 0.04 |

Table 2. Mechanical properties.

| S.No | PROPERTIES | RESULT |
|------|------------------|-------------------------|
| 1. | Tensile Strength | 430.02n/mm ² |
| 2. | Yield Strength | 390.62n/mm ² |
| 3. | Elongation | 4.81% |

The Cutting Tool

The turning operation has been carried out using multi-layer Al-Ti-N coated carbide insert using Physical Vapor Deposition – Thermal Evaporation Technique with specification as DNMG with 0.4 mm nose radius. Fig. 2 shows the schematic of multi-layer coated Carbide insert. A Right-hand side tool holder designated by ISO as PCLNR 2020 K12 was used for mounting the insert.



Figure 2. Multi-layer Al-Ti-N coated carbide insert using Thermal Evaporation Technique

The parameters chosen based on a literature survey and preliminary investigations in literatures. In total three parameters were considered, there are cutting speed, depth of cut and feed rate and the response parameters are surface roughness, interface temperature and cutting force.

In the present investigation Taguchi’s orthogonal array L9 was selected. The analysis of the experimental data was carried out MINITAB 14 software [7].

Table 3. Values of factors at different levels

| PARAMETERS | LEVELS | | |
|------------------------|--------|-----|-------|
| | L1 | L2 | L3 |
| cutting speeds (m/min) | 55 | 85 | 122 |
| depth of cut (mm) | 0.5 | 1 | 1.5 |
| Feed (mm/rev) | 0.1 | 0.2 | 0.315 |

ANALYSIS OF EXPERIMENTAL RESULTS

Factor effect on surface roughness

Table 4 and 5 shows the orthogonal array and experimental results with its corresponding S/N ratio.

Table 4 L9 Orthogonal Array and experimental data.

| Run | Cutting speed (m/min) | Depth of Cut (mm) | Feed (mm/rev) |
|-----|-----------------------|-------------------|---------------|
| 1 | 55 | 0.5 | 0.1 |
| 2 | 55 | 1 | 0.2 |
| 3 | 55 | 1.5 | 0.315 |
| 4 | 85 | 0.5 | 0.2 |
| 5 | 85 | 1 | 0.315 |
| 6 | 85 | 1.5 | 0.1 |
| 7 | 122 | 0.5 | 0.315 |
| 8 | 122 | 1 | 0.1 |
| 9 | 122 | 1.5 | 0.2 |

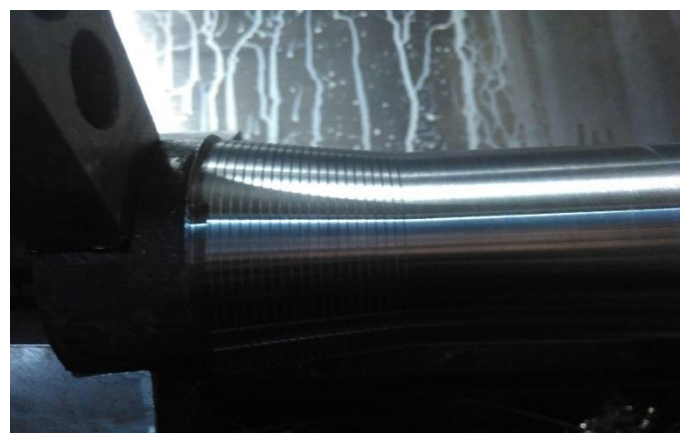


Figure 3. Hard turned ADI

Table 5. Experimental results.

| Run | SR | S/N Ratio (dB) | IT | S/N Ratio (dB) | CF | S/N Ratio (dB) |
|-----|------|----------------|-------|----------------|--------|----------------|
| 1 | 2.36 | -7.4582 | 32.16 | -30.1463 | 22.58 | 27.0745 |
| 2 | 1.27 | -2.0761 | 31.13 | -29.8636 | 20.81 | 26.3654 |
| 3 | 4.34 | -12.7498 | 56.43 | -35.0302 | 79.25 | 37.98 |
| 4 | 1.93 | -5.7111 | 34.03 | -30.6372 | 34.69 | 30.8041 |
| 5 | 2.48 | -7.889 | 41.03 | -32.262 | 61.97 | 35.8436 |
| 6 | 0.92 | 0.7242 | 34.23 | -30.6881 | 37.93 | 31.5797 |
| 7 | 2.08 | -6.3613 | 30.06 | -29.5598 | 12.601 | 22.0081 |
| 8 | 1.28 | -2.1442 | 31.23 | -29.8914 | 66.2 | 36.4172 |
| 9 | 1.27 | -2.0761 | 30.2 | -29.6001 | 63.28 | 36.0253 |

Table 6. Response Table for Signal to Noise Ratios Smaller is better

| Level | A | B | C |
|--------------|--------|--------|--------|
| 1 | -7.428 | -6.510 | -2.959 |
| 2 | -4.292 | -4.036 | -3.288 |
| 3 | -3.527 | -4.701 | -9.000 |
| DELTA | 3.901 | 2.474 | 6.041 |
| RANK | 2 | 3 | 1 |

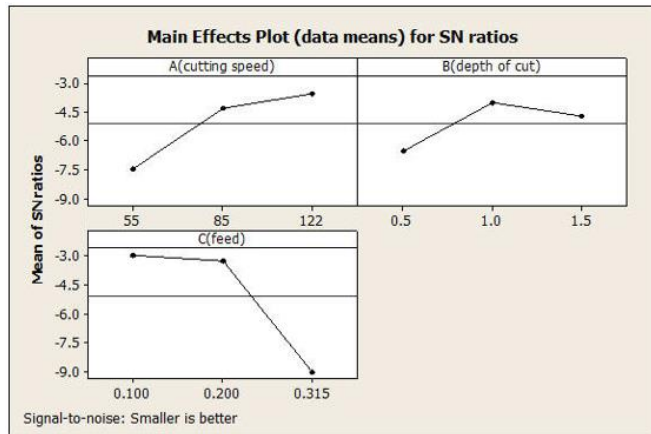


Figure 4. Main effect plots for S/N ratio

Based on the analysis of these experimental results with the help of signal to noise ratio, the optimum condition resulting in surface roughness is shown in the table 6 and figure 4. The figure clearly indicates that the third level of cutting speed, second level of depth of cut and first level of feed rate is optimum for surface roughness [12].

Factor effect on Interface Temperature

Table 7. Response Table for Signal to Noise Ratios Smaller is better

| Level | A | B | C |
|--------------|--------|--------|--------|
| 1 | -31.68 | -30.11 | -30.24 |
| 2 | -31.20 | -30.67 | -30.03 |
| 3 | -29.68 | -31.77 | -32.28 |
| DELTA | 2.00 | 1.66 | 2.25 |
| RANK | 2 | 3 | 1 |

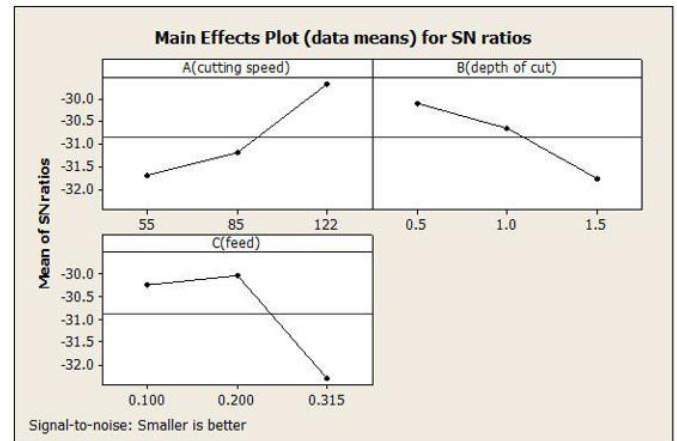


Figure 5. Main effect plots for S/N ratio

Based on the analysis of these experimental results with the help of signal to noise ratio, the optimum condition resulting in interface temperature is shown in the table 7 and figure 5. The figure clearly indicates that the third level of cutting speed, first level of depth of cut and second level of feed rate is optimum for interface temperature.

Factor effect on cutting force

Table 8. Response Table for Signal to Noise Ratios Larger is better

| Level | A | B | C |
|--------------|-------|-------|-------|
| 1 | 30.47 | 26.63 | 31.69 |
| 2 | 32.74 | 32.88 | 31.06 |
| 3 | 31.48 | 35.19 | 31.94 |
| DELTA | 2.27 | 8.57 | 0.88 |
| RANK | 2 | 1 | 3 |

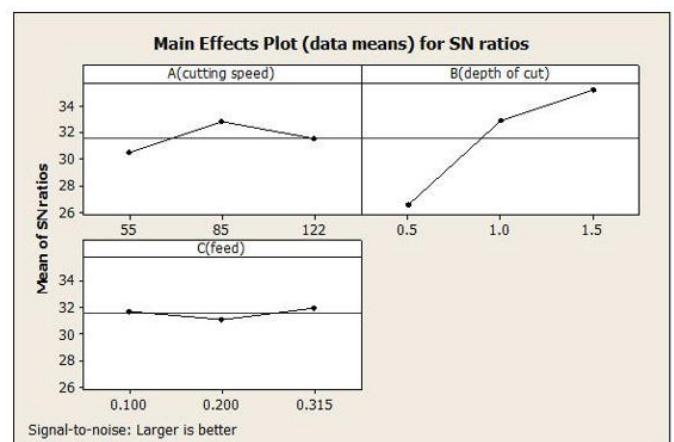


Figure 6. Main effect plots for S/N ratio

Based on the analysis of these experimental results with the help of signal to noise ratio, the optimum condition resulting in cutting force is shown in the table 8 and figure 6. The figure clearly indicates that the second level of cutting speed, third level of depth of cut and first level of feed rate is optimum for cutting force.

level of depth of cut and third level of feed rate is optimum for cutting force.

Regression Equation

The following regression equations were found using the least-square method in Minitab-R14 software. In this equation, following units are used to represent the parameters, cutting speeds (55,85,122 m/min), depth of cut (0.5,1,1.5 mm), and feed (0.1, 0.2 ,0.315 mm/rev).

The regression equation is

$$\text{Surface Roughness} = 1.95 - 0.0162 A (\text{cutting speed}) + 0.053 B (\text{depth of cut}) + 6.88 C (\text{feed})$$

R-Sq = 95.0% R-Sq(adj) = 93.1%

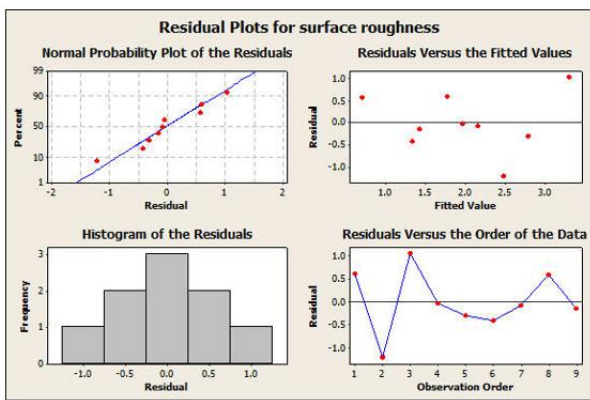


Figure 7. Residual plots for SR

The regression equation is

$$\text{Interface Temperature} = 30.0 - 0.141 A (\text{cutting speed}) + 8.20 B (\text{depth of cut}) + 47.5 C (\text{feed})$$

R-Sq = 92.4% R-Sq(adj) = 89.3%

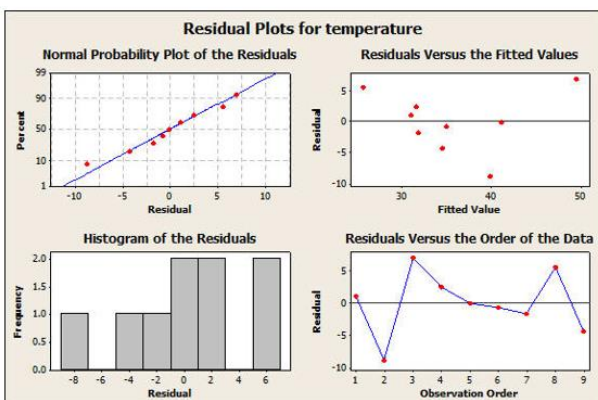


Figure 8. Residual plots for IT

The regression equation is

$$\text{Cutting Force} = - 9.8 + 0.096 A (\text{cutting speed}) + 36.9 B (\text{depth of cut}) + 43.5 C (\text{feed})$$

R-Sq = 96.3% R-Sq(adj) = 94.8%

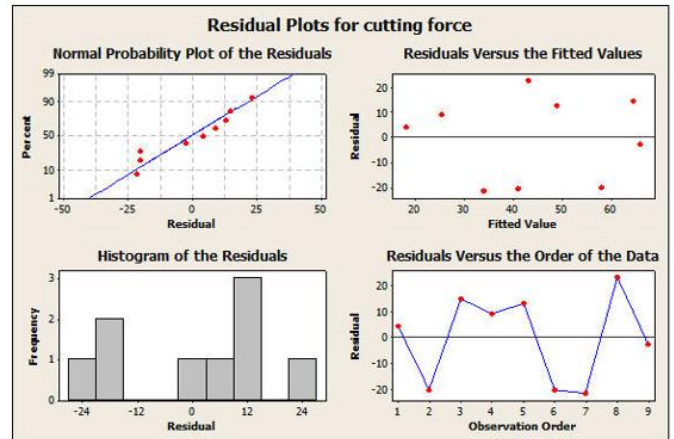


Figure 9. Residual plots for CF

Their R² values and adjusted R² values confirm the validity of the model as their values are above 90% for all the responses.

Confirmation test:

Confirmation test is the last step in analysis process and the parameter values for three different factors are shown in table 9 and the results of confirmation test are shown in table 10.

Table 9. Confirmation Experiment Parameters

| Factors | A | B | C |
|---------|----|---|-------|
| Value | 55 | 1 | 0.315 |

Table 10. Results of Confirmation Experiment

| Response | predicted | confirmatory |
|-----------------------|-----------|--------------|
| Surface Roughness | 3.27 | 3.12 |
| Interface Temperature | 45.40 | 44.52 |
| Cutting Force | 46.08 | 46.03 |

CONCLUSION:

This experiment was conducted to find the influence of the cutting speed, depth of cut and feed on the hard-turning performance characteristics of ADI material with coated insert. It was also tried to formulate a mathematical model for the responses such as SR, IT and CF. The conclusions from the analysis of these experimental results can be specified as follows:

1. Optimum surface roughness, interface temperature and cutting force obtained from the experiment, that the third level of cutting speed, second level of depth of cut and first level of feed rate are the optimum points. 4340 steel using uncoated and multilayer coated carbide inserts, Measurement 2012; 45, pp. 2153-2165.
2. The multiple regression equations for surface roughness, interface temperature and cutting force have been obtained.

REFERENCES

- [1] Hitchcox, AL, ADI has what it takes for high-performance gearing. Met. Prog 1986; 130 (2) 49-51.
- [2] Mohammed Seyed, Ali Boutorabi, Microstructures of austempered spheroidal graphite aluminium cast iron. Trans. Jpn Foundrym. Soc 1993; 12 .14-17.
- [3] Liu Qifu., 1993. Mechanism of spheroidal graphite formation in cast irons. Trans.Jpn Foundrym.Soc;12 18-24.
- [4] Bing-Qing Wei, Ji Liang, Wear-resistant bainite ductile iron and its strengthening mechanism. Trans. Jpn Foundrym.Soc 1993;12.62-68.
- [5] Chang, CH, Shih TS, Ausferrite transformation in austempered alloyed ductile irons. Trans. Jpn. Foundrym. Soc 1994;13 56-63.
- [6] Wang, CC et al, cutting austempered ductile iron using an EDM sinker. Journal of Mat. Proc. Tech 1999; 88. 83-89.
- [7] Dubensky, WJ, Rundman KB, An electron microscope study of carbide formation in ADI.AFS Trans 1985; 64-85,385-394.
- [8] Seah, KHW, Sharma SC, Machinability of alloyed Austempered ductile iron. Int. J. Mech. tools manufacturing 1995; Vol 35 No.10, pp1475-1479.
- [9] Kataoka, Y, Miyazaki T, Laser cutting of spheroidal graphite cast iron. Trans. Jpn. Foundrym. Soc 1993;12 37-44.
- [10] Chow, HM, Chang, MJ, Wang TJ, Cutting properties of austempered ductile iron. Conf. of Chinese fro casting, Taipei 1996; pp. 1-3.
- [11] Belgassim, O, Abusaada A, Investigation of the influence of EDM parameters on the overcut for AISI D3 tool steel. Proc IMechE, Part B: J Engineering Manufacture 2012; 226:365-370.
- [12] Choudhury, S.K., Jain, V.K. and Krishna, S.R., On-Line Monitoring of Tool Wear and Control of Dimensional Inaccuracy in Turning, Journal of Manufacturing Science Engineering 2001; 123, pp. 10-12.
- [13] Park, K. and Kwon, P.Y, Flank wears of multi-layer coated tool, Wear 2011; 270, pp. 771-780.
- [14] Sahoo, A. and Sahoo, B, Experimental investigation on machinability aspects in finish hard turning of AISI